

# Adaptive Risk Control for Social Navigation in Uncertain Crowded Environments

Xinyi Wang, Taekyung Kim, Bardh Hoxha, Georgios Fainekos and Dimitra Panagou

**Abstract**—Ensuring safety in crowded environments is challenging due to the inherent uncertainty in obstacle behavior. In this work, we propose an adaptive risk controller based on the Conditional Value-at-Risk Barrier Function (CVaR-BF), where the risk level is automatically adjusted to take the minimum necessary risk. This reduces the overly conservative influence of uncertainty estimation while maintaining robust performance in terms of safety and optimization feasibility. Additionally, we introduce a dynamic zone-based barrier function which characterizes the collision likelihood by evaluating the relative state between the robot and the obstacle. By integrating risk adaptation with this new function, our approach adaptively expands the safety margin, enabling the robot to proactively avoid obstacles in highly dynamic environments. Comparisons with baselines and different estimated uncertainty demonstrate that our method outperforms existing safe navigation approaches, and validate the effectiveness of our proposed framework.

## I. INTRODUCTION

Robot navigation in crowded, dynamic environments remains a fundamental challenge to safety specifications and actionable safe control due to “intangible” nature of obstacle uncertainty, such as awareness, reaction delay, or unpredictable motions. Conditional Value-at-Risk (CVaR), which quantifies the expected risk in the tail of a distribution, offers a principled way to manage such uncertainties [1]. Recent works successfully combine CVaR with Control Barrier Functions (CBFs) [2], [3] to enforce probabilistic safety constraints, e.g. [4]–[7]; However, performance of CVaR-Barrier Functions (CVaR-BF) based safety controllers heavily depends on accurately estimating the tail behavior of uncertainty distributions.

Many existing approaches quantify prediction uncertainty heuristically, often assuming Gaussian distributions or simplified agent models, failing to capture the complexity of real-world interactions [8]. Data-driven trajectory predictors such as RNNs or LSTMs typically provide no direct measure of uncertainty, increasing the risk of unsafe control decisions. Recent efforts have explored conformal prediction in [9], [10], to provide calibrated bounds on prediction errors from online data streams. While these methods offer theoretical guarantees and enhance safety margins, their inherent conservatism, especially when high confidence levels are

Xinyi Wang and Taekyung Kim are with the Department of Robotics, University of Michigan, Ann Arbor, MI, 48109, USA {xinywa, taekyung}@umich.edu

Bardh Hoxha and Georgios Fainekos are with the Toyota North America Research & Development, 1555 Woodridge Ave, Ann Arbor, MI 48105, USA {firstname.lastname}@toyota.com

Dimitra Panagou is with the Department of Robotics and the Department of Aerospace Engineering at University of Michigan, Ann Arbor, MI 48109, USA {dpanagou}@umich.edu

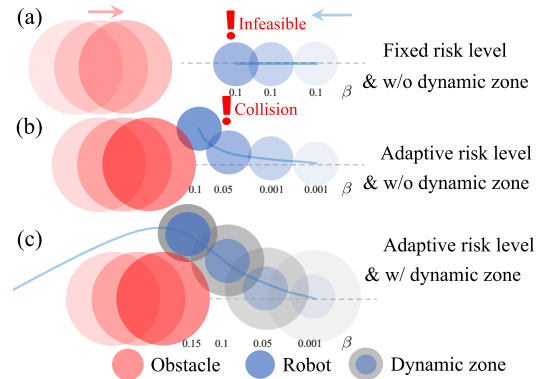


Fig. 1: Comparison of fixed vs adaptive risk levels with and without a dynamic zone.

required, can result in overly cautious controllers, often rendering the optimization problem infeasible in practice. This challenge highlights the need to design controller that can adaptively accommodate potential discrepancies between the actual distribution of obstacle motion and its predicted distribution.

Therefore, we propose a risk-adaptive navigation approach, a novel extension of the CVaR-BF framework that dynamically adjusts the risk level to maintain safety while ensuring trajectory feasibility. 1) Our controller integrates a conservative uncertainty quantification results to provide real-time bounds on obstacle motion uncertainty. Rather than relying on a fixed risk level, it begins with a risk-averse setting and incrementally increases the allowable risk until a feasible solution is obtained. This adaptive strategy enhances trajectory feasibility, mitigates the overly conservative influence of uncertainty estimation while ensuring CVaR safety is guaranteed at least a pre-defined threshold. 2) Besides, in highly dynamic scenarios, where obstacles move unpredictably and rapidly, the robot requires sufficient time and space to respond and adjust its risk level. overly conservative strategies can limit feasible solutions in crowded environments [11]–[13], so an approach that maintains safety without excessively restricting the decision space is essential. To this end, we introduce the concept of a “Dynamic Zone”, where the original safety distance is adaptively expanded based on the relative position and velocity between the robot and its surrounding obstacles. The robot adjusts its trajectory before nearing obstacles, but only when needed to avoid unnecessary conservatism, while also extending the risk-adaptive range.

## II. PRELIMINARIES

Consider a discrete-time control system:

$$\mathbf{x}_{k+1} = f(\mathbf{x}_k, \mathbf{u}_k), \quad (1)$$

where  $\mathbf{x}_k = [\mathbf{p}_k, \mathbf{v}_k]^T$  is the robot's state (position and velocity), and  $\mathbf{u}_k$  is the control input. Define the safe set given the obstacle states as

$$\mathcal{S} = \{\mathbf{x}_k \in \mathcal{X} : h(\mathbf{x}_k, \mathbf{x}_k^o) \geq 0\}. \quad (2)$$

$h : \mathcal{X} \times \mathcal{O} \rightarrow \mathbb{R}$  is the CBF that depends on both the system state  $\mathbf{x}_k$  and the obstacle state  $\mathbf{x}_k^o$ , where we assume perfect measurements of the states at the current time step  $k$ . However, the CBF at the next time step  $k+1$  considering the predicted state, which is denoted as  $h_{k+1} := h(\mathbf{x}_{k+1}, \hat{\mathbf{x}}_{k+1}^o)$ , becomes a random variable due to the uncertainty in the obstacle state  $\hat{\mathbf{x}}_{k+1}^o = g(\mathbf{x}_k^o) + \mathbf{w}_k$ , where  $\mathbf{w}_k$  represents stochastic disturbance. We sample noise  $\mathbf{w}_k$  in a finite set  $\mathcal{W} = \{\mathbf{w}^{(1)}, \mathbf{w}^{(2)}, \dots, \mathbf{w}^{(L)}\}$  with the probability mass function  $p_j, j \in \{1, \dots, L\}$ .  $\mathcal{W}$  can be estimated through some uncertainty qualification method, e.g., conformal prediction [10]. Then, the probabilistic safety condition requires that:

$$\mathbb{P}(h(\mathbf{x}_{k+1}, \hat{\mathbf{x}}_{k+1}^o) \geq 0) \geq 1 - \beta, \quad (3)$$

where  $\beta$  defines the risk level. A coherent risk measure capturing the expected loss in the worst-case tail of the distribution can be used to achieve this probabilistic constraint [14]:

$$\text{CVaR}_\beta(h_{k+1}) := \mathbb{E}[h_{k+1} \mid h_{k+1} \leq \text{VaR}_\beta(h_{k+1})] \geq 0. \quad (4)$$

Further extension of this constraint is using CVaR-BF [4]:

$$\text{CVaR}_\beta(h_{k+1}) \geq (1 - \gamma)h_k, \quad (5)$$

where  $0 < \gamma \leq 1$  controls the safety margin. We incorporate this constraint into an optimization to compute minimally invasive safe controls:

$$\min_{\mathbf{u}_k} \|\mathbf{u}_k - \bar{\mathbf{u}}_k\|^2 \quad \text{s.t.} \quad \text{CVaR}_\beta(h_{k+1}) \geq (1 - \gamma)h_k. \quad (6)$$

Note that the expectation in the CVaR formulation can be approximated by sampling noise [15], which offers robustness to non-Gaussian and heavy-tailed uncertainties. Therefore, the above optimization problem can be formulated as follows.

$$\begin{aligned} & \min_{\mathbf{u}_k \in \mathcal{U}, \zeta \in \mathbb{R}} \|\mathbf{u}_k - \bar{\mathbf{u}}_k\|^2 \\ & \text{s.t.} \quad -\left(\zeta + \frac{1}{\beta} \sum_{j=1}^L p_j [-h_{j,k+1} - \zeta]_+\right) \geq (1 - \gamma)h_k, \\ & \quad \forall j \in \{1, \dots, L\}. \end{aligned}$$

where  $\zeta$  is a real-valued auxiliary variable that searches for an optimal threshold.

## III. ADAPTIVE RISK LEVEL OF CVAR-BF

### A. Safety and Feasibility Analysis

We identify a key issue in CVaR-BF constraint: the tuning hyper-parameter, the risk level  $\beta$ , presents a trade-off between the safety and feasibility of the optimization problem in (6). **Safety Analysis:** (1) higher  $\beta$  relaxes the CVaR-BF constraint, allowing the robot to operate closer to obstacles, albeit at the expense of increased risk; (2) lower  $\beta$  enforces a tighter CVaR-BF constraint, yet may cause a higher chance of infeasibility and over-conservative decisions. **Feasibility Analysis:** Since the CVaR is monotonically increasing with respect to  $\beta$  according to its definition in (4), increasing  $\beta$  relaxes the safety constraint and consequently enlarges the feasible set. Therefore, if the safety constraints are too strict (small  $\beta$ ), the intersection of feasible space may be empty; if they are too loose (large  $\beta$ ), safety may be compromised.

### B. Adaptive Risk Level

Define the adaptive risk level at each time  $k$  as

$$\beta_k := \min\{\beta \in (0, \beta_u) \mid \mathcal{U}_\beta^k \neq \emptyset\}, \quad (7)$$

where  $\beta_u$  is the fixed risk level used in the standard CVaR formulation as in (4) and here we use it as the upper bound of the adaptive risk level.

**Definition 1** (Risk Adaptive CVaR Barrier Function). *Consider the discrete-time system (1) and an adaptive risk level  $\beta_k$  at each time step  $k$  as defined in (7). A function  $h : \mathbb{R}^n \rightarrow \mathbb{R}$  is called a Risk Adaptive CVaR Barrier Function for the safe set  $\mathcal{S}$  in (2) if there exists a constant  $\gamma \in (0, 1]$  such that for each  $\mathbf{x}_k \in \mathbb{R}^n$ , there exist a  $\mathbf{u}_k \in \mathbb{R}^m$  such that,*

$$\text{CVaR}_{\beta_k}^k(h_{k+1}) \geq (1 - \gamma)h_k, \quad \forall \mathbf{x}_k \in \mathcal{X}. \quad (8)$$

The notion of the risk adaptive CVaR barrier function allows to initialize the risk level with a conservative value (close to zero), and then incrementally increase it when necessary. A trade-off is needed only when the robot nears obstacles, while risk level remains low elsewhere to maintain a high probability of safety throughout the trajectory, achieving higher CVaR-safety.

**Theorem 1** (CVaR-Safety with Adaptive Risk Level). *Consider the discrete-time system (1) and the safe set  $\mathcal{S}$  (2). Let  $\beta_u \in (0, 1)$  be a fixed upper-bound risk level, and let  $\beta_k \in (0, \beta_u]$  be an adaptive risk level at time  $k$  as defined in (7). Then,  $\mathcal{S}$  is at least CVaR-safe with respect to the risk level  $\beta_u$  if there exists a risk adaptive CVaR barrier function as defined in Definition 1.*

## IV. DYNAMIC SAFETY ZONES FOR CVAR BARRIER FUNCTIONS

Effective risk management is essential for robotic navigation, particularly in environments with high-speed obstacles and uncertainties that shorten reaction times and increase collision risks. Fig. 1a shows that using a fixed risk level can render the problem infeasible when the robot approaches an obstacle. In contrast, Fig. 1b employs an adaptive risk

level (as described in Sec. III-B) that starts conservatively prompting the robot to initiate a turn early, and then relaxes the safety requirements as needed. However, without incorporating a dynamic zone that provides a virtual radius (an extra buffer), this risk adjustment can ultimately compromise safety and lead to collisions. Therefore, as shown in Fig. 1c, the combination of an adaptive risk level with a dynamic zone not only facilitates early obstacle avoidance but also provides greater flexibility for risk adjustments, thereby relaxing constraints and expanding the feasible space.

#### A. Dynamic Zone-Based Barrier Function

Classical CBFs typically rely on a distance-based measure, denoted as  $h^D$ , that may lead to myopic behavior, causing the robot to navigate too close to obstacles and thereby increasing the risk of collision. Functions based on velocity obstacles or collision cones [11]–[13], denoted as  $h^C$ , incorporate the relative motion between the robot and the obstacle, which can be overly conservative, rendering the navigation problem infeasible [13]. Define a dynamic zone-based barrier function that leverages the predicted relative state:

$$h_k^Z := \|\mathbf{p}_k - \mathbf{p}_k^o\|^2 - R_{\text{safe}}^2(1 + \Delta_k),$$

$$\Delta_k = \left( -\frac{\langle \mathbf{p}_k^{\text{rel}}, \mathbf{v}_k^{\text{rel}} \rangle}{\|\mathbf{p}_k^{\text{rel}}\| \|\mathbf{v}_k^{\text{rel}}\|} \right)_+, \quad (9)$$

where  $(\cdot)_+$  denotes the nonnegative part, i.e.,  $\max\{0, \cdot\}$ , ensuring that  $\Delta_k \in [0, 1]$ . Instead of imposing a direct constraint on the relative angle which can lead to unnecessary obstacle avoidance when the robot is far away [13], our approach modulates the safety zone only when necessary. When the robot and obstacles are far apart, even if the safety zone radius is expanded, it does not significantly influence the robot's behavior due to the large relative distance. Thus, this strategy prevents unnecessary avoidance of obstacles and avoids the overly conservative behavior that can result from rigid angle constraints.

#### B. Probabilistic Safety Guarantee

We further can get the conclusion that a dynamic zone-based barrier function expands the adjustment space of the  $\beta_k$  value, while also ensuring that the given risk level  $\beta_u$  is met. The key insight is that the dynamic zone represents a larger, dynamic, yet virtual safety distance, rather than the actual physical separation between the robot and an obstacle (see Fig. 1c).

**Lemma 1** (Equivalence of Probabilistic Safety Guarantee). *Given a safe set  $S$  (2) that is CVaR-safe under the risk adaptive CVaR-BF defined in Definition 1 with the distance-based barrier function  $h^D$  and a fixed risk level upper bound  $\beta_u$ . Then, by adopting the dynamic zone-based barrier function  $h^Z$  together with the newly derived upper bound  $\bar{\beta}_u$  for the adaptive risk level, the resulting safety guarantee is equivalent to that provided by the original CVaR-BF. In other words, the safe set  $S$  remains CVaR-safe with the same probabilistic guarantee.*

## V. SIMULATIONS

### A. Experimental Setup

1) *Agent Settings*: We evaluate our proposed method using a widely adopted crowd navigation simulation environment within a 12 m  $\times$  12 m space [16] (see Fig. 2). Obstacles are modeled using a single-integrator dynamic system with position uncertainty:  $\hat{\mathbf{p}}_{k+1}^o = \mathbf{p}_{k+1}^o + \mathbf{w}_{p,k}$ , where  $\mathbf{w}_{p,k} \sim \mathcal{N}(\mathbf{0}, \Sigma_p)$ , with  $\Sigma_p = \text{diag}(\sigma^2, \sigma^2)$  representing the position noise covariance. We vary the uncertainty level by setting  $\sigma \in \{0.0, 0.025, 0.05, 0.075, 0.15\}$ , and simulate  $\mathbf{w}_{p,k}$  within  $\pm 3\sigma$  per axis. We let the obstacles follow the *uncooperative behavior*, same settings with work in [17], meaning it only avoids collisions with other obstacles. Their maximum speeds along each axis are chosen uniformly from  $\{0.3, 0.6, 0.9, 1.2\}$  m/s, and their radii are selected from  $\{0.3, 0.4, 0.5\}$  m. The robot is modeled as a double integrator, with dynamics given by For each axis, the maximum acceleration is restricted to be less than 3 m/s<sup>2</sup>, and the maximum velocity is limited to under 2 m/s. The time step is set to  $\Delta t = 0.1$  s. The local sensor range is 5 m. The results can be found in the video here.

### B. Benchmark Comparisons

We first test our method with assuming accurate estimated uncertainties distributions: a normal distributed around zero mean with standard deviation same with simulated noise. We compare our method with the following baselines:

- 1) CVaR-BF Methods: distance-based CVaR-BF with fixed risk levels ( $\beta = 0.01$  or  $0.99$ ) [4] (*CVaR(Dist)*).
- 2) CBF Methods: collision cone-based approaches [11], including a robust control for worst-case scenarios (*RCBF(Cone)*) and a standard CBF-based control without explicit uncertainty handling (*CBF(Cone)*).
- 3) RL Methods: socially attentive reinforcement learning (*CrowdNav*) [16] and its extension incorporating predicted obstacle intentions (*CrowdNav++*) [17].
- 4) Geometric Methods: reciprocal velocity obstacles for collision-free motion (*ORCA*) [1].

### C. Impact of Uncertainty Estimation

We then evaluate how different estimated uncertainty bounds affect controller performance. Following the approach in [4], we consider a uniform distribution over a bounded disturbance set  $\mathcal{W}$  for  $\mathbf{w}_{p,k}$ . While  $\mathcal{W}$  can be estimated online using uncertainty quantification techniques [10], we fix it as a conservative bounded region in this simulations to isolate and validate the impact of our proposed adaptive risk controller. In next step work, we will incorporate real-time uncertainty estimation to dynamically bound obstacle motion uncertainty to further verify the performance of our risk adaptive controller.

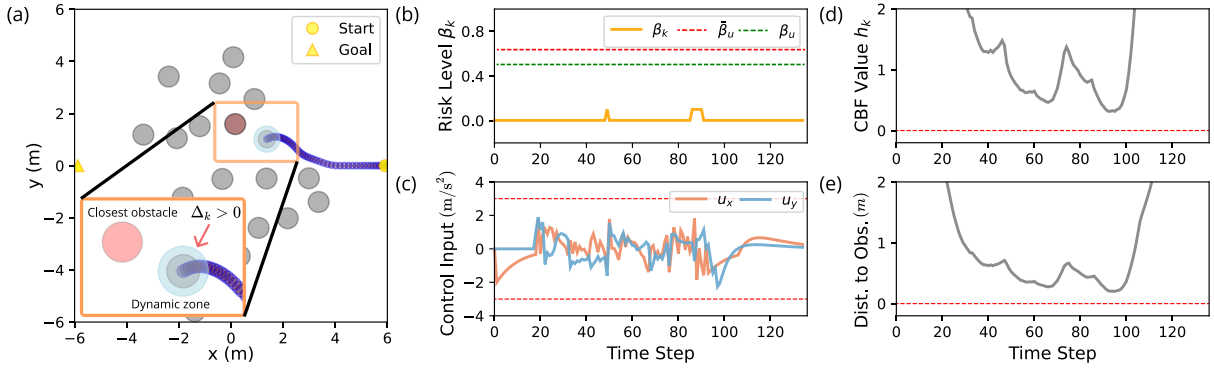


Fig. 2: Visualization of robot trajectories and associated metrics for the whole trajectory in an environment with 20 uncooperative obstacles. (a) Snapshot of the trajectory at a critical time step. (b) Risk level  $\beta_k$  over time. (c) Control input over time. (d) CBF value over time (e) Distance to closest obstacle over time. In (a), when the robot and an obstacle approach each other with high relative velocity, the dynamic safety margin will expand, i.e.,  $\Delta_k > 0$  making robot proactively avoid obstacles. As shown in (b),  $\beta_k$  will also increase where feasible space is limited, but it remains below the upper bound  $\bar{\beta}_u$ , ensuring safety without being overly conservative. (e) shows robot maintains a safe distance from obstacles due to dynamic zone-based barrier function.

## REFERENCES

- [1] J. Alonso-Mora, A. Breitenmoser, M. Ruffi, P. Beardsley, and R. Siegwart, "Optimal reciprocal collision avoidance for multiple non-holonomic robots," in *Distributed autonomous robotic systems*. Springer, 2013, pp. 203–216.
- [2] A. D. Ames, S. Coogan, M. Egerstedt, G. Notomista, K. Sreenath, and P. Tabuada, "Control barrier functions: Theory and applications," in *European Control Conference (ECC)*, 2019, pp. 3420–3431.
- [3] K. Garg, J. Usevitch, J. Breeden, M. Black, D. Agrawal, H. Parwana, and D. Panagou, "Advances in the theory of control barrier functions: Addressing practical challenges in safe control synthesis for autonomous and robotic systems," *Annual Reviews in Control*, vol. 57, p. 100945, 2024.
- [4] M. Ahmadi, X. Xiong, and A. D. Ames, "Risk-averse control via cvar barrier functions: Application to bipedal robot locomotion," *IEEE Control Systems Letters*, vol. 6, pp. 878–883, 2021.
- [5] M. Kishida, "A risk-aware control: Integrating worst-case cvar with control barrier function," *arXiv preprint arXiv:2308.14265*, 2023.
- [6] S. Safaoui and T. H. Summers, "Distributionally robust cvar-based safety filtering for motion planning in uncertain environments," in *IEEE International Conference on Robotics and Automation (ICRA)*, 2024, pp. 103–109.
- [7] T. Kim, R. I. Kee, and D. Panagou, "Learning to refine input constrained control barrier functions via uncertainty-aware online parameter adaptation," *IEEE International Conference on Robotics and Automation (ICRA)*, 2025.
- [8] S. H. Nair, V. Govindarajan, T. Lin, C. Meissen, H. E. Tseng, and F. Borrelli, "Stochastic mpc with multi-modal predictions for traffic intersections," in *2022 IEEE 25th International Conference on Intelligent Transportation Systems (ITSC)*. IEEE, 2022, pp. 635–640.
- [9] A. Dixit, L. Lindemann, S. X. Wei, M. Cleaveland, G. J. Pappas, and J. W. Burdick, "Adaptive conformal prediction for motion planning among dynamic agents," in *Learning for Dynamics and Control Conference*. PMLR, 2023, pp. 300–314.
- [10] J. Zhang, S. Z. Yong, and D. Panagou, "Safety-critical control with offline-online neural network inference," *arXiv preprint arXiv:2408.00918*, 2024.
- [11] M. Tayal, R. Singh, J. Keshavan, and S. Kolathaya, "Control barrier functions in dynamic uavs for kinematic obstacle avoidance: A collision cone approach," in *American Control Conference (ACC)*. IEEE, 2024, pp. 3722–3727.
- [12] A. Haraldsen, M. S. Wiig, A. D. Ames, and K. Y. Pattersen, "Safety-critical control of nonholonomic vehicles in dynamic environments using velocity obstacles," in *American Control Conference (ACC)*. IEEE, 2024, pp. 3152–3159.
- [13] A. S. Roncero, R. I. C. Muchacho, and P. Ögren, "Multi-agent obstacle avoidance using velocity obstacles and control barrier functions," *arXiv preprint arXiv:2409.10117*, 2024.
- [14] R. T. Rockafellar and S. Uryasev, "Optimization of conditional value-at-risk," *Journal of risk*, vol. 2, pp. 21–42, 2000.
- [15] S. Sarykalin, G. Serraino, and S. Uryasev, "Value-at-risk vs. conditional value-at-risk in risk management and optimization," in *State-of-the-art decision-making tools in the information-intensive age*. Informis, 2008, pp. 270–294.
- [16] C. Chen, Y. Liu, S. Kreiss, and A. Alahi, "Crowd-robot interaction: Crowd-aware robot navigation with attention-based deep reinforcement learning," in *IEEE International Conference on Robotics and Automation (ICRA)*, 2019, pp. 6015–6022.
- [17] S. Liu, P. Chang, Z. Huang, N. Chakraborty, K. Hong, W. Liang, D. L. McPherson, J. Geng, and K. Driggs-Campbell, "Intention aware robot crowd navigation with attention-based interaction graph," in *IEEE International Conference on Robotics and Automation (ICRA)*, 2023, pp. 12 015–12 021.